Nickel phosphide nanoalloy catalyst for the selective deoxygenation of sulfoxides to sulfides under ambient H_2 pressure

Shu Fujita,[a] Sho Yamaguchi,[a] Seiji Yamazoe,[b] Jun Yamasaki,[c] Tomoo Mizugaki[a] and Takato Mitsudome*[a]

[a] Department of Materials Engineering Science, Graduate School of Engineering Science, Osaka University, 1-3 Machikaneyama, Toyonaka, Osaka 560-8531, Japan

E-mail: mitsudom@cheng.es.osaka-u.ac.jp

[b] Department of Chemistry, Tokyo Metropolitan University, 1-1 Minami Osawa, Hachioji, Tokyo 192-0397, Japan

[c] Research Center for Ultra-High Voltage Electron Microscopy, Osaka University, 7-1, Mihogaoka, Ibaraki, Osaka 567-0047, Japan

Abstract

Exploring novel catalysis by less common, metal–non-metal nanoalloys is of great interest in organic synthesis. We herein report a titanium-dioxide-supported nickel phosphide nanoalloy (nano-Ni_2P/TiO_2) that exhibits high catalytic activity for the deoxygenation of sulfoxides. nano-Ni_2P/TiO_2 deoxygenated various sulfoxides to sulfides under 1 bar of H_2, representing the first non-noble metal catalyst for sulfoxide deoxygenation under ambient H_2 pressure. Spectroscopic analyses revealed that this high activity is due to cooperative catalysis by nano-Ni_2P and TiO_2.

KEYWORDS: nickel phosphide, heterogeneous catalyst, deoxygenation, sulfoxide, titanium dioxide

Introduction

It is well known that metal–metal nanoalloys often exhibit unique physicochemical properties that are superior to those of nanocrystals comprised of individual metals.[1,2] In the field of catalysis, significant

enhancements in activity, selectivity, and/or durability have been made by alloying two or more metals.[3–5] In contrast, further extension beyond the use of traditional metal–metal nanoalloys to novel catalysis by metal–non-metal nanoalloys has not yet been widely explored. Recently, the rapid advance of nanoengineering technology has enabled the precise synthesis and catalytic application of metal–non-metal nanoalloys. Accordingly, metal–non-metal nanoalloys, e.g., metal phosphide nanoalloys, have been gaining attention as electrocatalysts for energy conversion reactions[6–8] and petroleum-reforming catalysts for hydrotreating reactions.[9–11] However, despite this catalytic potential, the catalytic applications of metal phosphide nanoalloys for the organic synthesis of fine and bulk chemicals are less developed.[12–18] In this context, our research group has recently focused on exploring the novel catalysis by metal phosphide nanoalloys, finding that non-noble metal phosphide nanoalloy catalysts can outperform conventional metal nanoparticles for hydrogenation reactions.[19,20] For instance, a nickel phosphide nanoalloy (nano-Ni_2P) represents the first example of a non-noble metal catalyst for the selective hydrogenation of biofuranic aldehydes to diketones in water.[19] In addition, a cobalt phosphide nanoalloy (nano-Co_2P) exhibits outstanding catalytic performance for nitrile hydrogenation, with 20–500-fold greater activity than previously reported non-noble metal catalysts.[20] Thus, catalysis by metal phosphide nanoalloys for liquid-phase molecular transformations represents an exciting research area that still has unexplored possibilities, especially for organic synthesis.

The deoxygenation of sulfoxides is an important transformation in organic synthesis because sulfoxides are utilized as chirons in asymmetric transformations.[21–24] A target chiral compound can be synthesized through a series of reactions including the introduction of a chiral sulfoxide and its subsequent deoxygenation. To date, many stoichiometric methods using metal hydrides,[25–27] hydrogen halides,[28–30] thiols,[31,32] and phosphines[33–35] have been reported for the deoxygenation of sulfoxides. Alternative catalytic methods employing Mo, Re, Cu, Au, and Ru combined with phosphorus compounds,[36–38] hydrosilanes,[39–41] BH_3,[42–44] and alcohols[45–47] have been also developed. However, these catalytic systems still suffer from low atom efficiency. In contrast, the catalytic deoxygenation of sulfoxides with H_2 represents the most environmentally friendly method for the synthesis of sulfides with high atom efficiency because water is formed as the sole by-product.[48–53] Our research group recently found that Ru/TiO_2 has a high catalytic activity for the deoxygenation of various sulfoxides under ambient H_2 pressure.[48] Subsequently, Pt-MoO_x/TiO_2,[49] $Pt/V_{0.7}Cr_{0.3}$-Hol,[50] and Pt/H_xMoO_{3-y}[51] catalysts were developed. As alternatives to expensive and rare noble-metal-based catalysts, low-cost and earth-abundant non-noble metal catalysts for the deoxygenation of sulfoxides have been also

developed. In this context, only two non-precious metal catalysts have been reported for the deoxygenation of sulfoxides using H_2.[52,53] One is a high-valent oxo-molybdenum(VI) complex catalyst which requires harsh reaction conditions (50 bar H_2, 120 °C).[52] The other is a Co-Mo/NC catalyst which operates well at room temperature but requires pressurized H_2 (10 bar) and a long reaction time (60 h) to obtain sufficient sulfide yields.[53] Therefore, the development of a new and efficient catalytic system based on a non-precious metal catalyst operating under mild conditions would greatly advance the utility of sulfoxide deoxygenation. Herein, we report that a titanium-dioxide-supported nickel phosphide nanoalloy (nano-Ni_2P/TiO_2) exhibits high catalytic activity for the deoxygenation of sulfoxides to sulfides using H_2 (Scheme 1). In contrast to the previously reported non-noble metal catalysts requiring high H_2 pressures, nano-Ni_2P/TiO_2 is the first example of a non-noble metal catalyst that promotes the selective deoxygenation of various sulfoxides to the corresponding sulfides under ambient H_2 pressure.

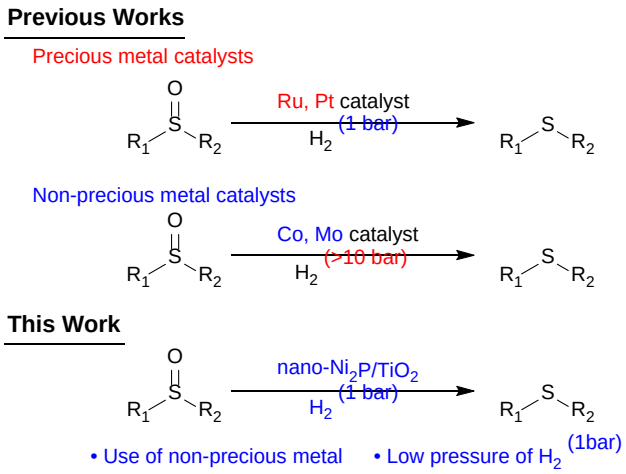

Scheme 1 Catalytic deoxygenation of sulfoxides to sulfides using H_2.

Results and discussion

nano-Ni_2P was synthesized by a solvothermal method using nickel(II) chloride ($NiCl_2$) and triphenyl phosphite as the nickel and phosphorous precursors, respectively.[19] For comparison, nano-Co_2P and nano-Fe_2P were prepared by similar methods (Fig. S1 and S2). The formation of nano-Ni_2P was evidenced by X-ray diffraction (XRD). In the XRD pattern of nano-Ni_2P (Fig. S1), the diffraction peaks located at 2θ = 40.8°, 44.7°, 47.3°, and 54.1° can be ascribed to the (111), (201), (210), and (300) planes of Ni_2P (JCPDS card no. 03-0953), respectively.[54] Fig. 1a shows a transmission electron

microscopy (TEM) image of a collection of spherical nano-Ni_2P particles, which have a mean diameter of 5.2 nm. A high-magnification TEM image shows the well-resolved lattice fringes of nano-Ni_2P (Fig. 1b), where the lattice spacings of 0.236 and 0.224 nm correspond to the (102) and (111) planes of hexagonal Ni_2P, respectively (Fig. 1c and 1d).[55] Moreover, the selected area electron diffraction (SAED) pattern is consistent with that of hexagonal Ni_2P (inset, Fig. 1b), which further verifies the formation of crystalline Ni_2P.[56] Next, nano-Ni_2P was immobilized on TiO_2. nano-Ni_2P was dispersed in hexane and then stirred with TiO_2, giving nano-Ni_2P/TiO_2. The high dispersion of nano-Ni_2P on TiO_2 was also confirmed, as depicted in Fig. 1e. These results clearly showed the successful immobilization of uniform and crystalline nano-Ni_2P on TiO_2.

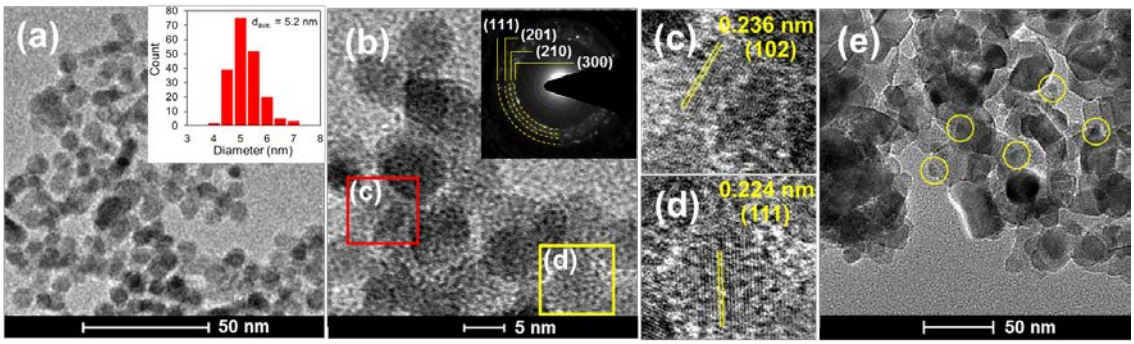

Fig. 1 a) TEM image and histogram of nano-Ni_2P. b) High-magnification TEM image of nano-Ni_2P (the inset in (b) shows the corresponding SAED pattern). c) and d) Enlarged views of the area selected by the red and yellow square in (b), respectively. e) TEM image of nano-Ni_2P/TiO_2 with nano-Ni_2P marked in yellow circles.

We initially assessed the catalytic potential of various metal phosphide nanoalloys for the deoxygenation of diphenyl sulfoxide (**1a**) under 10 bar of H_2 at 120 °C for 1 h, as summarized in Table 1. nano-Ni_2P promoted the deoxygenation of **1a**, affording diphenyl sulfide (**2a**) in 14% yield (entry 1). In contrast, other non-noble metal phosphides, namely, nano-Co_2P, nano-Fe_2P, and bulk Ni_2P, showed almost no activity (entries 2–4), revealing the unique deoxygenation catalysis by nano-Ni_2P. Next, active nano-Ni_2P immobilized on various supports, such as TiO_2, ZrO_2, Nb_2O_5, SiO_2, hydrotalcite (HT), and Al_2O_3, were tested for the deoxygenation of **1a** (entries 5, 9–13). While most of the supported Ni_2P alloys provided **2a** in yields similar to or lower than that with unsupported nano-Ni_2P, nano-Ni_2P/TiO_2 and nano-Ni_2P/ZrO_2 had 2–3-fold higher activities, giving **2a** in 33% and 28% yields, respectively (entries 5 and 9). These results showed that the combination of the Ni_2P nanoalloy

with TiO_2 provides the best activity among the tested metal phosphide nanoalloy catalysts, suggesting that metal–support cooperation plays an important role in the present deoxygenation reaction. With nano-Ni_2P/TiO_2 in hand, the reaction conditions were optimized. When 4A molecular sieves (4Å M.S.) were added to remove the water generated during the reaction, the yield of **2a** was further improved to 56% with a reaction time of 1 h and reached 98% when the reaction time was extended to 2.5 h (Table 1, entries 6 and 7). Notably, with nano-Ni_2P/TiO_2, the reaction proceeded under just 1 bar of H_2, providing **2a** in 97% yield (Table 1, entry 8). This is the first example of sulfoxide deoxygenation using a non-precious metal catalyst under ambient H_2 pressure.

Next, we carried out a hot filtration experiment using nano-Ni_2P/TiO_2 to confirm the occurrence of hydrogenation on the catalyst surface. After the removal of nano-Ni_2P/TiO_2 by filtration at approximately 50% conversion of **1a**, no further conversion was observed (Fig. S3). In addition, the concentration of Ni in the filtrate was below the detection limit of inductively coupled plasma atomic emission spectrometry (ICP-AES), and the Ni loading amount of used nano-Ni_2P/TiO_2 was almost the same as that of the fresh catalyst (Table S1). These results showed that nano-Ni_2P was strongly immobilized on the TiO_2 support and there was no leaching of Ni species from the catalyst, indicating that this is the active species for the deoxygenation of sulfoxides.

Table 1 Deoxygenation of diphenyl sulfoxide (**1a**) catalyzed by metal phosphide catalysts[a]

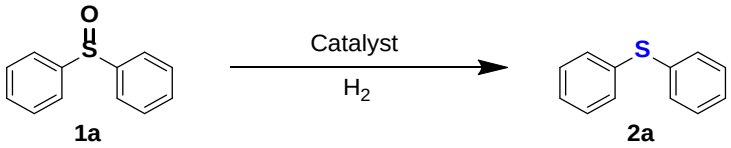

Entry	Catalyst	Time (h)	Yield (%)[b]
1	nano-Ni_2P	1	14
2	nano-Co_2P	1	<1
3	nano-Fe_2P	1	<1
4	bulk Ni_2P	1	<1
5	nano-Ni_2P/TiO_2	1	33
6[c]	nano-Ni_2P/TiO_2	1	56
7[c]	nano-Ni_2P/TiO_2	2.5	98
8[d]	nano-Ni_2P/TiO_2	12	97
9	nano-Ni_2P/ZrO_2	1	28

10	nano-Ni_2P/Nb_2O_5	1	15
11	nano-Ni_2P/SiO_2	1	11
12	nano-Ni_2P/HT	1	10
13	nano-Ni_2P/Al_2O_3	1	8

[a] Reaction conditions: catalyst (5 mol% metal), **1a** (0.5 mmol), toluene (3 mL), H_2 (10 bar), 120 °C. [b] Determined by gas chromatography-mass spectrometry (GC-MS) using naphthalene as an internal standard. [c] 4Å M.S. (0.1 g). [d] 4Å M.S. (0.1 g), H_2 (1 bar), 160 °C.

The substrate scope of the sulfoxide deoxygenation reaction catalyzed by nano-Ni_2P/TiO_2 under atmospheric H_2 was investigated (Scheme 2). nano-Ni_2P/TiO_2 efficiently promoted the selective deoxygenation of various sulfoxides, including aromatic (**2a**–**2e**) and aliphatic (**2f**–**2i**) substrates, giving the corresponding sulfides in high yields. Notably, functional groups such as halogens (**2j** and **2k**), ether (**2l**), carbonyls (**2m** and **2n**), and alkene (**2o**) were tolerated because nano-Ni_2P/TiO_2 operated under mild conditions. In particular, selective deoxygenation of sulfoxide while retaining an aldehyde group was achieved for the first time, with nano-Ni_2P/TiO_2 chemoselectively deoxygenating 4-(methylsulfinyl)benzaldehyde to the corresponding 4-(methylthio)benzaldehyde (**2m**). Furthermore, nano-Ni_2P/TiO_2 was applicable to the gram-scale reaction: 1.0 g of **1a** was successfully converted to **2a** with a yield of 92%, where a turnover number (TON) reached 92 (Scheme 3). This value of TON is significantly larger than those of previously reported non-noble metal catalyst systems (Table S3). This result demonstrates that the nano-Ni_2P/TiO_2 shows high catalytic activity and durability for the deoxygenation of sulfoxides. Conclusively, the use of nano-Ni_2P/TiO_2 provides a powerful method for the selective deoxygenation of various functionalized sulfoxides to the corresponding sulfides under ambient H_2 conditions.

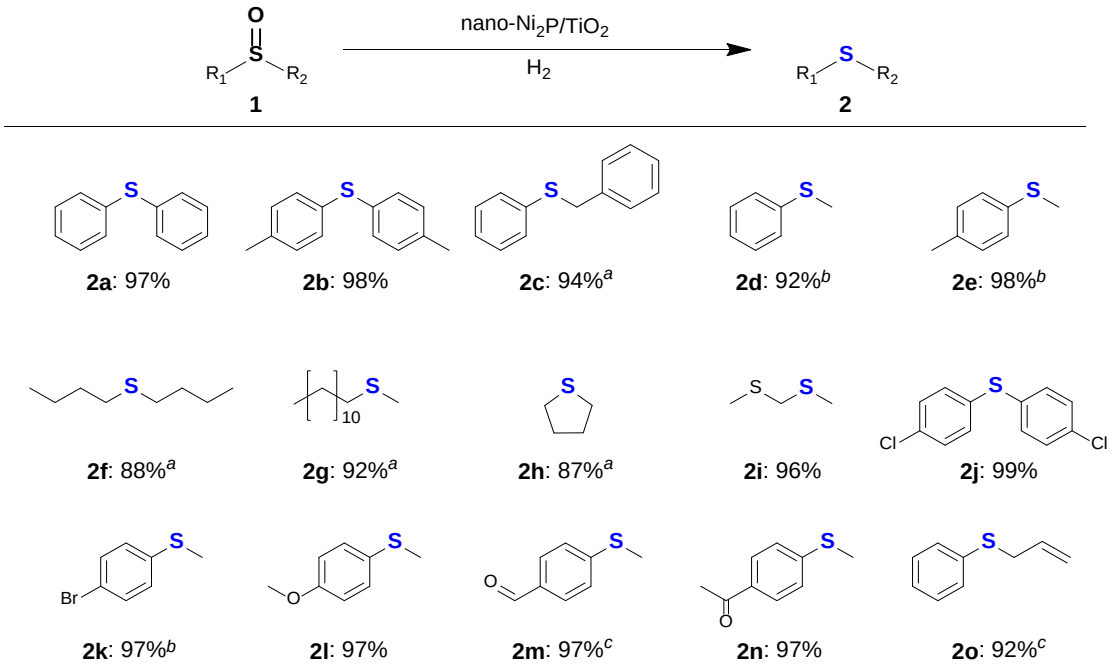

Scheme 2 Deoxygenation of various sulfoxides catalyzed by nano-Ni_2P/TiO_2. Reaction conditions: nano-Ni_2P/TiO_2 (0.145 g, 5 mol% Ni), substrate (0.5 mmol), toluene (3 mL), 4Å M.S. (0.1 g), H_2 (1 bar), 160 °C, 12 h. Yields were determined by GC-MS using naphthalene as an internal standard. [a] 10 mol% Ni, 140 °C. [b] 10 mol% Ni. [c] 10 mol% Ni, 120 °C, 24 h.

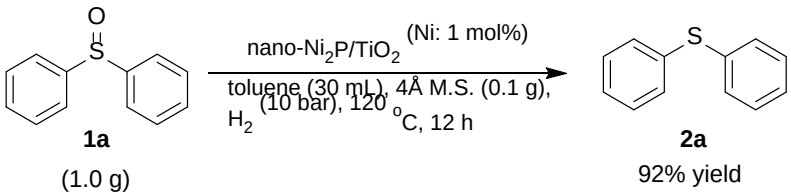

Scheme 3 Gram-scale reaction of diphenyl sulfoxide using nano-Ni_2P/TiO_2.

X-ray absorption fine structure (XAFS) analysis was used to investigate the structure–activity relationship of nano-Ni_2P/TiO_2. The X-ray absorption near-edge structure (XANES) spectra of Ni foil, NiO, nano-Ni_2P, and nano-Ni_2P/TiO_2 measured in air are shown in Fig. 2. The absorption edge energy of nano-Ni_2P (Fig. 2, red line) is close to that of Ni foil (Fig. 2, blue line), which indicates that the Ni species in nano-Ni_2P are in a metallic state.[19] Further, the absorption edge energy of nano-Ni_2P/TiO_2 (Fig. 2, green line) is similar to that of nano-Ni_2P, suggesting that the Ni species in nano-Ni_2P retain their metallic nature after immobilization on TiO_2. However, slight changes in the spectral features of

nano-Ni_2P/TiO_2 suggest that TiO_2 affects the local structure and/or electronic state of nano-Ni_2P. Hence, the nano-Ni_2P/TiO_2 catalyst has an air-stable metallic nature that is active for hydrogenation, unlike conventional nickel(0) catalysts such as Raney Ni which are oxidatively degraded in the atmosphere.[57] The Fourier transform of the extended XAFS (FT-EXAFS) spectrum of nano-Ni_2P showed two peaks at 1.7 and 2.3 Å, which are assigned to Ni–P and Ni–Ni bonds, respectively (Fig. S4).[58,59] The absence of Ni–O bonds indicated that nano-Ni_2P is not oxidized, which is consistent with the XANES analysis. Curve-fitting analysis suggested that the Ni–Ni bond length of nano-Ni_2P (2.58 Å) was longer than that of Ni foil (2.48 Å) owing to the formation of vertex-sharing NiP_4 tetrahedra. Interestingly, nano-Ni_2P was significantly different from bulk Ni_2P, in terms of the coordination number (*CN*) ratio, with the $CN_{Ni–Ni}/CN_{Ni–P}$ ratio of nano-Ni_2P (1.0) being smaller than the ideal value in bulk Ni_2P (3.3) (Fig. S5 and Table S2). This small value for the $CN_{Ni–Ni}/CN_{Ni–P}$ ratio in nano-Ni_2P indicates the presence of highly coordinatively unsaturated Ni–Ni sites on the surface which can activate H_2.[14,19] The crystal structure of Ni_2P and an exposed (300) plane are shown in Fig. S6. We infer that the lower $CN_{Ni–Ni}/CN_{Ni–P}$ ratio of nano-Ni_2P is due to the exposure of the (300) plane because many Ni–Ni sites are arranged on this plane. Hence, the difference between the deoxygenation activities of nano-Ni_2P and bulk Ni_2P is derived from the highly coordinatively unsaturated active sites for H_2 on the exposed (300) plane of nano-Ni_2P.

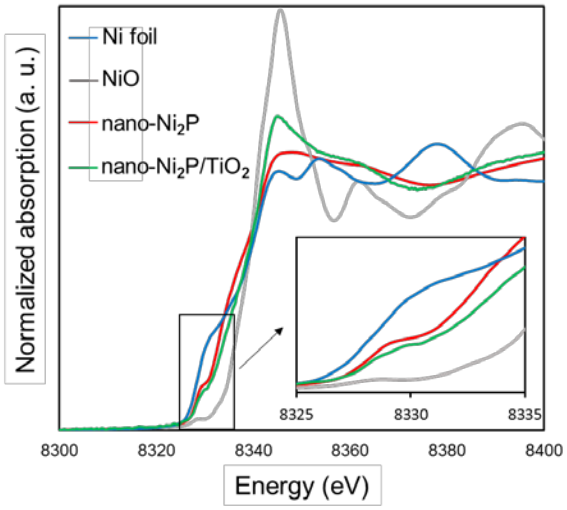

Fig. 2 Ni *K*-edge XANES spectra of Ni foil, NiO, nano-Ni_2P, and nano-Ni_2P/TiO_2.

Next, X-ray photoelectron spectroscopy (XPS) measurements of nano-Ni_2P were carried out. The

Ni 2p XPS spectrum of nano-Ni_2P showed two peaks located at 853.1 and 870.2 eV, which were similar to those of metallic Ni $2p_{3/2}$ (852.8 eV) and Ni $2p_{1/2}$ (870.0 eV) (Fig. S7), supporting the metallic nature of the Ni species in nano-Ni_2P. Furthermore, XPS measurements of nano-Ni_2P/TiO_2 were performed to elucidate the role of TiO_2 in the deoxygenation of sulfoxides. Fig. 3 shows the Ti 2p XPS spectrum of nano-Ni_2P/TiO_2, where the Ti $2p_{3/2}$ peak located at 458.8 eV corresponds to Ti^{4+} of TiO_2 (Fig. 3a). After treating nano-Ni_2P/TiO_2 under deoxygenation conditions without sulfoxides (10 bar H_2 at 120 °C for 1 h), a peak assigned to Ti^{3+} appeared at 458.2 eV, suggesting that Ti^{4+} species on TiO_2 is partially reduced to Ti^{3+} accompanied by the formation of oxygen vacancy (O_v) sites (Fig. 3b).[60,61] Furthermore, the Ti^{3+} peak disappeared by the subsequent treatment of nano-Ni_2P/TiO_2 with **1a** in toluene under an argon atmosphere (Fig. 3c), resulting in the production of **2a** (Scheme S1). This result indicated that the in situ generated Ti^{3+} species are oxidized by sulfoxide, that is, the O_v sites on TiO_2 could deoxygenate **1a** to **2a**.

Based on these results, we proposed a reaction pathway for the deoxygenation of sulfoxides catalyzed by nano-Ni_2P/TiO_2 through the cooperative behavior of nano-Ni_2P and TiO_2 (Scheme 4). First, H_2 is activated at a coordinatively unsaturated Ni–Ni site on nano-Ni_2P (**I**). Subsequently, the spillover hydrogen diffuses onto the TiO_2 surface (**II**), where it reduces TiO_2 to form an O_v site (**III**).[62,63] The O_v site in TiO_2 deoxygenates the sulfoxide to give a sulfide (**IV**), thereby completing the catalytic cycle. The cooperative effects of nano-Ni_2P and TiO_2 play key roles in the activation of H_2 followed by the formation of O_v sites and the deoxygenation of sulfoxide, respectively. This hybrid catalysis system leads to the high performance of nano-Ni_2P/TiO_2 in the deoxygenation of sulfoxides.

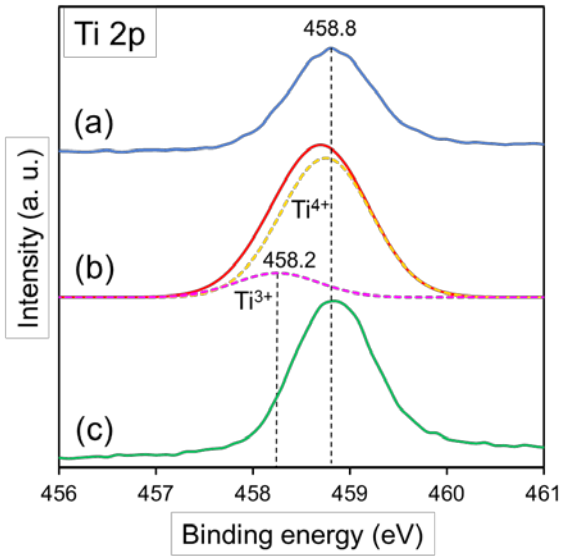

Fig. 3 Ti 2p XPS spectra of a) nano-Ni_2P/TiO_2, b) (a) after treatment with H_2, and c) (b) after treatment with **1a**. The curve-fitted data are shown as dash lines in (b).

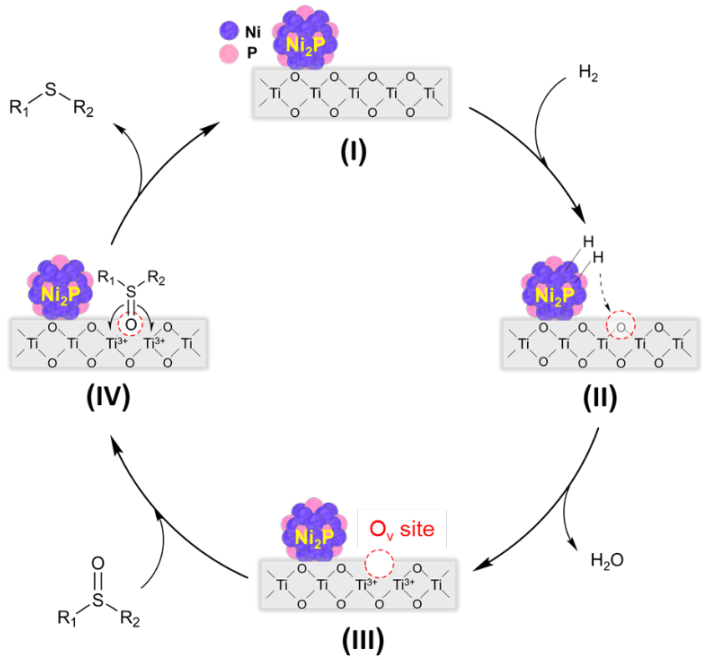

Scheme 4 Proposed reaction pathway for the deoxygenation of sulfoxides through the cooperative catalysis by nano-Ni_2P and TiO_2 support.

Conclusion

We found that a TiO_2-supported Ni_2P nanoalloy efficiently promoted the selective deoxygenation of sulfoxides to sulfides under mild conditions. This system is the first non-precious metal catalyst to achieve sulfoxide deoxygenation to sulfides under just 1 bar of H_2. A wide variety of sulfoxides bearing reducible functional groups were chemoselectively converted to the corresponding sulfides in high yields while retaining the functional groups. XAFS and XPS analyses revealed that the Ni_2P nanoalloy and TiO_2 efficiently and cooperatively functioned to activate H_2 and deoxygenate the sulfoxide, respectively, leading to high catalytic performance. These results confirm the potential of metal phosphide nanoalloys for catalysing a wide variety of molecular transformations under mild conditions. We envisage that our study will make a significant contribution to expand the unexplored catalytic potential of metal phosphide nanoalloys for organic synthesis.

Experimental section

General information

X-ray diffraction (XRD) studies were conducted on a Philips X′Pert-MPD diffractometer with Cu-Kα radiation. Transmission electron microscopy (TEM) was carried out FEI Tecnai G2 20ST instruments operating at 200 kV. Gas chromatography–mass spectrometry (GC-MS) was performed using a GCMS-QP2010 SE instrument equipped with an inert Cap WAX-HT capillary column (30 m × 0.25 mm i.d.). The oven temperature was programmed as follows: Starting temperature of 100 °C held for 2 min, then ramped to 280 °C at 20 °C /min. Ni *K*-edge X-ray absorption spectra were recorded at room temperature using a Si (111) monochromator at the BL01B1 line of SPring-8 at the Japan Synchrotron Radiation Research Institute (JASRI), Harima, Japan. The obtained spectra were analyzed using Athena software. After normalization at edge height, the k^3-weighted χ spectra were extracted. XPS analysis was performed on a KRATOS system equipped with a mono Al X-ray source and a hemispherical analyzer operating in the fixed analyzer transmission mode. The spectra were obtained at a pass energy of 40.0 eV with an Al-K X-ray source operating at 50 W and 154 kV. The analysis area was 0.7 × 0.3 mm^2 while the working pressure in the analysis chamber was less than 1 × 10^{-8} Pa. The C 1s peak at a binding energy of 285.0 eV was used as the internal reference.

General procedure for the synthesis of nano-Ni_2P/TiO_2

All reactions were conducted under an argon atmosphere using standard Schlenk line techniques. In a typical synthesis, $NiCl_2·6H_2O$ (1.0 mmol) was combined with hexadecylamine (10 mmol) and triphenyl phosphite (10 mmol) in a Schlenk flask. The mixture was stirred at 120 °C for 1 h. Subsequently, increasing the temperature to 315 °C while stirring gave a black colloidal solution. The mixture was allowed to cool down to room temperature and the black product was then collected by centrifugation. The obtained powder was washed with a chloroform–acetone mixture (1:1, v/v) and dried in vacuo overnight to give nano-Ni_2P. Next, nano-Ni_2P (22 mg) was dispersed in hexane (100 mL) with sonication for 1 h and then stirred with TiO_2 (1.0 g) for 6 h at room temperature. The obtained powder was dried in vacuo overnight to give nano-Ni_2P/TiO_2 as a grey powder. Similar procedures were used to prepare the other nano-Ni_2P/support (ZrO_2, Nb_2O_5, SiO_2, HT, and Al_2O_3) catalysts.

Typical catalytic reaction

As a representative catalytic reaction, the transformation of **1a** to **2a** using nano-Ni_2P/TiO_2 was typically performed as follows. First, nano-Ni_2P/TiO_2 (0.145 g) and 4Å M.S. (0.1 g) were placed in a 50 mL stainless-steel autoclave with a Teflon inner cylinder, followed by the addition of **1a** (0.5 mmol) and toluene (3 mL). The reaction mixture was stirred vigorously at 120 °C under 10 bar of H_2. The

reaction solution was then analyzed by GC-MS to determine the conversion and yield using naphthalene as an internal standard method.

Conflicts of interest

The authors declare that they have no competing interests.

Acknowledgments

This work was supported by JSPS KAKENHI Grant Nos. 17H03456, 17H03457, 18H01790, and 20H02523. A part of this work was supported by the Cooperative Research Program of the Institute for Catalysis, Hokkaido University (20B1027) and the Nanotechnology Open Facilities in Osaka University (A-19-OS-0060), Ministry of Education, Culture, Sports, Science and Technology (MEXT), Japan. We thank Dr. Yoshikata Nakajima (Institute for NanoScience Design, Osaka University) for the TEM observation and Dr. Toshiaki Ina (SPring-8) for the XAFS measurements (2019A1390, 2019A1649, 2019B1560, and 2020A1487).

Notes and references

[1] K. D. Gilroy, A. Ruditskiy, H.-C. Peng, D. Qin and Y. Xia, *Chem. Rev*., 2016, **116**, 10414–10472.

[2] M. Sankar, N. Dimitratos, P. J. Miedziak, P. P. Wells, C. J. Kiely and G. J. Hutchings, *Chem. Soc. Rev*., 2012, **41**, 8099–8139.

[3] H. Fang, J. Yang, M. Wen and Q. Wu, *Adv. Mater*., 2018, **30**, 1705698.

[4] W. Luo, M. Sankar, A. M. Beale, Q. He, C. J. Kiely, P. C. Bruijnincx and B. M. Weckhuysen, *Nat. Commun.*, 2015, **6**, 6540.

[5] L. Kesavan, R. Tiruvalam, M. H. Ab Rahim, M. I. bin Saiman, D. I. Enache, R. L. Jenkins, N. Dimitratos, J. A. Lopez-Sanchez, S. H. Taylor, D. W. Knight, C. J. Kiely and G. J. Hutchings, *Science*, 2011, **331**, 195–199.

[6] Y. Li, Z. Dong and L. Jiao, *Adv. Energy Mater.*, 2020, **10**, 1902104.

[7] Y. Shi and B. Zhang, *Chem. Soc. Rev.*, 2016, **45**, 1529–1541.

[8] Y. Lv and X. Wang, *Catal. Sci. Technol*., 2017, **7**, 3676–3691.

[9] M. C. Alvarez-Galvan, J. M. Campos-Martin and J. L. G. Fierro, *Catalysts*, 2019, **9**, 293.

[10] S. T. Oyama, *J. Catal.*, 2003, **216**, 343–352.

[11] S. T. Oyama, T. Gott, H. Zhao and Y.-K. Lee, *Catal. Today*, 2009, **143**, 94–107.

[12] D. Albani, K. Karajovic, B. Tata, Q. Li, S. Mitchell, N. López and J. Pérez-Ramírez, *ChemCatChem*, 2019, **11**, 457–464.

[13] Y. Zhu, S. Yang, C. Cao, W. Song and L.-J. Wan, *Inorg. Chem. Front.*, 2018, **5**, 1094–1099.

[14] R. Gao, L. Pan, H. Wang, X. Zhang, L. Wang and J.-J. Zou, *ACS Catal.*, 2018, **8**, 8420–8429.

[15] S. Yang, L. Peng, E. Oveisi, S. Bulut, D. T. Sun, M. Asgari, O. Trukhina and W. L. Queen, *Chem. – Eur. J.*, 2018, **24**, 4234–4238.

[16] J.-J. Shi, H.-J. Feng, C.-L. Qv, D. Zhao, S.-G. Hong and N. Zhang, *Appl. Catal., A*, 2018, **561**, 127–136.

[17] Y. Chen, C. Li, J. Zhou, S. Zhang, D. Rao, S. He, M. Wei, D. G. Evans and X. Duan, *ACS Catal.*, 2015, **5**, 5756–5765.

[18] S. Carenco, A. Leyva-Pérez, P. Concepción, C. Boissière, N. Mézailles, C. Sanchez and A. Corma, *Nano Today*, 2012, **7**, 21–28.

[19] S. Fujita, K. Nakajima, J. Yamasaki, T. Mizugaki, K. Jitsukawa and T. Mitsudome, *ACS Catal.*, 2020, **10**, 4261–4267.

[20] T. Mitsudome, M. Sheng, A. Nakata, J. Yamasaki, T. Mizugaki and K. Jitsukawa, *Chem. Sci.*, 2020, **11**, 6682–6689.

[21] S. C. A. Sousa and A. C. Fernandes, *Coord. Chem. Rev.*, 2015, **284**, 67–92.

[22] M. C. Carreño, *Chem. Rev.*, 1995, **95**, 1717–1760.

[23] M. Madesclaire, *Tetrahedron*, 1988, **44**, 6537–6580.

[24] P. Bravo, G. Resnati, F. Viani and A. Arnone, *Tetrahedron*, 1987, **43**, 4635–4647.

[25] J. Drabowicz and M. Mikołajczyk, *Synthesis*, 1976, 527–528.

[26] S. Kano, Y. Tanaka, E. Sugino and S. Hibino, *Synthesis*, 1980, 695–697.

[27] J. Zhang, X. Gao, C. Zhang, C. Zhang, J. Luan and D. Zhao, *Synth. Commun.*, 2010, **40**, 1794–1801.

[28] T. Aida, N. Furukawa and S. Oae, *Tetrahedron Lett.*, 1973, **14**, 3853–3856.

[29] D. Landini, A. M. Maia and F. Rolla, *J. Chem. Soc., Perkin Trans. 2*, 1976, 1288–1291.

[30] J. T. Doi and W. K. Musker, *J. Am. Chem. Soc.*, 1981, **103**, 1159–1163.

[31] T. J. Wallace and J. J. Mahon, *J. Am. Chem. Soc.*, 1964, **86**, 4099–4103.

[32] B. Karimi and D. Zareyee, *Synthesis*, 2003, 1875–1877.

[33] I. W. J. Still, S. K. Hasan and K. Turnbull, *Can. J. Chem.*, 1978, **56**, 1423–1428.

[34] S. Kikuchi, H. Konishi and Y. Hashimoto, *Tetrahedron*, 2005, **61**, 3587–3591.

[35] Y. Jang, K. T. Kim and H. B. Jeon, *J. Org. Chem.*, 2013, **78**, 6328–6331.

[36] Z. Zhu and J. H. Espenson, *J. Mol. Catal. A*, 1995, **103**, 87–94.

[37] R. Sanz, J. Escribano, R. Aguado, M. R. Pedrosa and F. J. Arnáiz, *Synthesis*, 2004, 1629–1632.

[38] M. Bagherzadeh, M. M. Haghdoost, M. Amini and P. G. Derakhshandeh, *Catal. Commun.*, 2012, **23**, 14–19.

[39] S. C. A. Sousa, J. R. Bernardo, M. Wolff, B. Machura and A. C. Fernandes, *Eur. J. Org. Chem.*, 2014, 1855–1859.

[40] S. Enthaler, *ChemCatChem*, 2011, **3**, 666–670.

[41] Y. Mikami, A. Noujima, T. Mitsudome, T. Mizugaki, K. Jitsukawa and K. Kaneda, *Chem. – Eur. J.* 2011, **17**, 1768–1772.

[42] A. C. Fernandes and C. C. Romão, *Tetrahedron Lett.*, 2007, **48**, 9176–9179.

[43] S. Enthaler, S. Krackl, E. Irran and S. Inoue, *Catal. Lett.*, 2012, **142**, 1003–1010.

[44] D. J. Harrison, N. C. Tam, C. M. Vogels, R. F. Langler, R. T. Baker, A. Decken and S. A. Westcott, *Tetrahedron Lett.*, 2004, **45**, 8493–8496.

[45] N. García, P. García-García, M. A. Fernández-Rodríguez, R. Rubio, M. R. Pedrosa, F. J. Arnáiz and R. Sanz, *Adv. Synth. Catal.*, 2012, **354**, 321–327.

[46] N. García, P. García-García, M. A. Fernández-Rodríguez, D. García, M. R. Pedrosa, F. J. Arnáiz and R. Sanz, *Green Chem.*, 2013, **15**, 999–1005.

[47] Y. Takahashi, T. Mitsudome, T. Mizugaki, K. Jitsukawa and K. Kaneda, *Chem. Lett.*, 2014, **43**, 420–422.

[48] T. Mitsudome, Y. Takahashi, T. Mizugaki, K. Jitsukawa and K. Kaneda, *Angew. Chem., Int. Ed.*, 2014, **53**, 8348–8351.

[49] A. S. Touchy, S. M. A. H. Siddiki, W. Onodera, K. Kon and K. Shimizu, *Green Chem.*, 2016, **18**, 2554–2560.

[50] T. Uematsu, Y. Ogasawara, K. Suzuki, K. Yamaguchi and N. Mizuno, *Catal. Sci. Technol.*, 2017, **7**, 1912–1920.

[51] Y. Kuwahara, Y. Yoshimura, K. Haematsu and H. Yamashita, *J. Am. Chem. Soc.*, 2018, **140**, 9203–9210.

[52] P. M. Reis, P. J. Costa, C. C. Romão, J. A. Fernandes, M. J. Calhorda and B. Royo, *Dalton Trans.*, 2008, 1727–1733.

[53] K. Yao, Z. Yuan, S. Jin, Q. Chi, B. Liu, R. Huang and Z. Zhang, *Green Chem.*, 2020, **22**, 39–43.

[54] Y. Feng, C. Xu, E. Hu, B. Xia, J. Ning, C. Zheng, Y. Zhong, Z. Zhang and Y. Hu, *J. Mater. Chem. A*, 2018, **6**, 14103–14111.

[55] D. Yang, Y. Gu, X. Yu, Z. Lin, H. Xue and L. Feng, *ChemElectroChem*, 2018, **5**, 659–664.

[56] Y. Ni, L. Jin and J. Hong, *Nanoscale*, 2011, **3**, 196–200.

[57] D. Shi, R. Wojcieszak, S. Paul and E. Marceau, *Catalysts*, 2019, **9**, 451.

[58] H. Zhao, S. T. Oyama, H.-J. Freund, R. Włodarczyk and M. Sierka, *Appl. Catal., B*, 2015, **164**, 204–216.

[59] H.-R. Seo, K.-S. Cho and Y.-K. Lee, *Mater. Sci. Eng., B*, 2011, **176**, 132–140.

[60] H. Huang, H. Huang, P. Hu, X. Ye and D. Y. C. Leung, *Int. J. Photoenergy*, 2013, **2013**, 350570.

[61] P. Li, X. Guo, S. Wang, R. Zang, X. Li, Z. Man, P. Li, S. Liu, Y. Wu and G. Wang, *J. Mater. Chem. A*, 2019, **7**, 2553–2559.

[62] M. Lu, Y. Sun, P. Zhang, J. Zhu, M. Li, Y. Shan, J. Shen and C. Song, *Ind. Eng. Chem. Res.*, 2019, **58**, 1513–1524.

[63] P. Zhang, Y. Sun, M. Lu, J. Zhu, M. Li, Y. Shan, J. Shen and C. Song, *Energy Fuels*, 2019, **33**, 7696–7704.